OPEN

PRS GLOBAL OPEN

ORIGINAL ARTICLE
Research

Finite Element Analysis of the Stress Changes Associated With the Growth of Acne Keloids

Nobuaki Ishii, MD*†
Satoshi Akaishi, MD, PhD†‡
Masataka Akimoto, MD, PhD*†
Shizuko Ichinose, PhD†
Satoshi Usami, PhD§
Teruyuki Dohi, MD, PhD†¶
Rei Ogawa, MD, PhD, FACS†¶

Background: Almost half of all spontaneously occurring keloids are acne keloids on the anterior chest. These keloids often grow in a crab-claw shape due to predominant tractional stresses on the scar; such stresses are risk factors for keloid growth/progression. To understand the relationship between acne keloid growth and mechanical stress, we conducted finite element analysis (FEA), measured the long/short dimensions of photographed acne keloids, and subjected acne keloids to microscopy.

Methods: FEA was conducted on 10 identically shaped ellipsoidal keloids whose long-axis length rose from 5 to 50 mm in 5-mm increments. They were embedded in the skin and subjected to traction. The stress on the keloid and its surrounding tissues was determined. Dimensions of 220 acne keloids were measured. Electron/light microscopy was conducted on the center, margins, and surrounding tissues of chest acne keloids.

Results: FEA showed that as the keloid "grew," the tractional stress centered on its core, then became evenly distributed, and then focused increasingly on the tractioned keloid margin, especially its shallow dermis. This is associated with increasing stress in the surrounding tissues at the keloid margin. Clinical dimension measurements showed that acne keloids remained round until 4–5 mm, after which they elongated rapidly. Electron microscopy showed that in the surrounding skin, fragments of keratinocyte, fibrin, and numerous cell fragments were observed just below the epidermal basement membrane.

Conclusions: Keloid-prone acne should be treated with steroid tape or other keloid therapy when it reaches 4–5 mm in diameter. *(Plast Reconstr Surg Glob Open 2024; 12:e6365; doi: 10.1097/GOX.0000000000006365; Published online 20 December 2024.)*

INTRODUCTION

Keloids are pathological dermatofibroproliferative scars that grow relentlessly beyond the borders of the original damaged area. They originate from burns, surgery, acne, folliculitis, and even insect bites that induce inflammation in the reticular dermis. They are associated with itching and pain, have an unappealing appearance, and are highly refractory to monotherapies. They are the result of aberrant chronic prolongation of the inflammatory phase of wound healing, which induces excessive deposition of extracellular matrix by fibroblasts and angiogenic hyperplasia.[1,2] The inflammation is driven by genetic, systemic (eg, sex hormones), and local factors, including mechanical forces on the margins of the wounded/scarred skin. The evidence for the latter risk factor includes the predilection of keloids for body areas that are subject to strong/repetitive mechanical stresses (eg, the anterior chest) and the characteristic shapes of keloids on specific body areas: these reflect the predominant directions of the local mechanical forces and include the crab claw on the chest, the butterfly on the shoulder, and the dumbbell on the upper arm.[2–14] Mechanobiological and observational studies suggest that mechanical stimuli may drive inflammation by activating local mechanosensitive cells, including endothelial cells and fibroblasts.[15–17]

*From the *Department of Plastic Surgery, Nippon Medical School Chibahokusoh Hospital, Inzai City, Chiba Prefecture, Japan; †Department of Plastic, Reconstructive and Regenerative Surgery, Graduate School of Medicine, Nippon Medical School, Bunkyo Ward, Tokyo, Japan; ‡Department of Plastic Surgery, Nippon Medical School Musashikosugi Hospital, Kawasaki City, Kanagawa Prefecture, Japan; §Graduate School of Education, University of Tokyo, Bunkyo Ward, Tokyo, Japan; and ¶Department of Plastic, Reconstructive and Aesthetic Surgery, Nippon Medical School, Bunkyo Ward, Tokyo, Japan.*

Received for publication September 12, 2024; accepted October 11, 2024.

DOI: 10.1097/GOX.0000000000006365

Disclosure statements are at the end of this article, following the correspondence information.

However, because a reliable animal model of keloid formation and progression is lacking, it has been difficult to study how mechanical stress drives keloid growth. Consequently, several studies have instead used finite element analysis (FEA).[18–20] This method evaluates the force-induced displacement of all points of the structure under study at the resolution of a linear system[21] and has shown that body movement–induced stretching tension on keloids in the chest region stresses the keloid at its leading edges. The skin around the keloids is also stressed, as shown by inflammation, proliferation, and upregulation of the caveolin-1/ROCK mechanotransduction pathway. These changes are thought to be driven by the disparate stiffness of the keloid, which is filled with thick collagen ropes and is therefore inflexible, and the softer surrounding skin. The alterations in the surrounding skin may ultimately promote the horizontal growth of the inflamed keloid margin into the surrounding skin.[18–20]

Almost half of all naturally occurring (ie, noniatrogenic) keloids arise from acne on the anterior chest.[6] These keloids are likely initiated by acne-induced inflammation and tissue damage (erosion and ulceration) in the reticular dermis[22]; this inflammation in combination with other keloid risk factors (eg, genetics and sex hormones) leads to chronic keloidogenic inflammation. It is thought that mechanical forces then drive the growth of the small round acne keloids, causing them to adopt the classical crab-claw shape. To examine this further, we here explored the role of mechanical stress in the conversion of small acne keloids into elongating keloids that spread into the surrounding skin with (1) FEA, (2) length and width measurements of 220 acne-derived keloids on keloid-prone body regions of patients, and (3) electron and light microscopic analyses of acne-derived chest keloids.

Takeaways

Question: How does the distribution of traction-induced stress on acne keloids change as the keloids grow?

Findings: Our finite element analysis showed that tractional stress initially stressed the keloid core, but as the keloid "grew," the stress became initially equally distributed all over the keloid and subsequently focused intensely at the shallow dermis of the keloid at its tractioned edge.

Meaning: The key to treating acne keloids is to reduce the inflammation in the shallow dermis of the keloid margins by steroid taping or other means.

METHODS

This study consisted of 3 substudies: (1) FEA, where traction was placed on a 5-mm-long ellipsoid keloid and 9 other identically shaped keloids that were 5 mm longer than the preceding keloid. The effect of traction on the distribution of stress on the keloid and the surrounding skin, and how this changed with increasing keloid size, was then determined. (2) Measurements of the long and short diameters of acne keloids in patients to determine the keloid-size threshold where acne keloids start to elongate. (3) Electron and light microscopy of an excised acne-derived chest keloid specimen to determine the tissue changes in the keloid center, margin, and surrounding tissues. The study protocol was approved by the institutional review board of Nippon Medical School Hospital (Approval No. M-2023-158) and was conducted in accordance with the Declaration of Helsinki.

Finite Element Analysis

Finite Element Modeling

FEA was performed using Fusion 360 (Autodesk) software. The finite element modeling consisted of a 10 × 10 cm^2 of full-thickness skin. On the basis of the reported thickness of the skin on the chest, shoulders, and back,[23] the epidermis, dermis, and subcutaneous adipose tissue thicknesses were set at 0.1, 1.5, and 20 mm, respectively. A keloid body was modeled in the center of the square such that it was buried within the dermal layer. The keloid was oblate spheroid in shape, with an ellipse rotated around the short axis, which is the height. To represent a growing keloid, 10 models were created: in the first, the keloid body was 5 mm in major axis diameter and the next 9 models were 5 mm longer than the preceding keloid, such that the last keloid was 50 mm in major axis diameter. All models had the same aspect ratio: the major axis, which is the width, and the minor axis, which is the height (50:7). The heights of these keloids changed proportionally and ranged from 0.7 to 7 mm. Each model was divided into 4 sections through the center of the keloid body. Because each of the 4 partitioned models was symmetrical, 4 partitioned models were used for simulation for each size.

Simulation

The models were constructed with the following physical properties, which were based on the literature[18–20,24]: (1) Young modulus values of 0.003, 0.002, and 0.004 GPa were used for the epidermis/dermis, subcutaneous tissue, and keloid, respectively; and (2) Poisson ratio of 0.49 was used for all tissues. The model was meshed into 1-mm^3 microstructures. The bottom of 4 partitioned models and 2 sides through the keloid center were constrained. To stress the keloid, it was subjected to 100 N traction in a unilateral direction along its long axis. The distribution of von Mises stress on the keloid body and the surrounding tissues was then observed.

Measuring Dimensions of Acne-derived Keloids From Patients

All patients with erythematous and elevated acne keloids on the chest, shoulders, and/or back who visited our outpatient clinic from June to September 2023 were included. The clinical photographs of keloids of all candidate were retrieved, and their long and short diameters were measured. Keloids that were close to each other and clearly affected each other's morphology or were fused were excluded. The data were presented as 2-dimensional scatterplots with long and short diameters on the horizontal and vertical axes, respectively. We also performed a

linear regression analysis. The scatterplots were also converted to contour lines to visualize the number of individuals of each size.

Pathological Study

One anterior chest-acne-derived keloid that was excised was prepared for light microscopy with toluidine-blue staining and electron microscopy. The keloid center, leading keloid margin, and surrounding tissue were observed separately. Thus, the tissue specimen was fixed for 2 hours with 2.5% glutaraldehyde in 0.1 M phosphate buffer, fixed with 1% osmium tetroxide buffered with 0.1 M phosphate buffer for 2 hours, dehydrated with a graded series of ethanol, embedded in Epon 812, sliced into semithin (1-µm-thick), and stained for 30 seconds with toluidine blue. Light microscopy (BZ9000; Keyence, Osaka, Japan) was then conducted. Some of the sections obtained for light microscopy were thinned further into ultrathin sections (80- to 90-nm-thick), placed on copper grids, double-stained with uranyl acetate and lead citrate, and then examined with a transmission electron microscope (JEM-1400plus; JEOL, Tokyo, Japan).

RESULTS

FEA of a Keloid at Various Growth Stages That Was Subjected to Traction

The distribution of von Mises stress on the keloid body and the surrounding tissues was then observed. Simulation results for the model with the keloid embedded in the skin show stresses on the surrounding tissue and on the core of the keloid (Figs. 1A–5A). In addition, each keloid body was exposed, and the stresses on the surface of the keloid body were observed (Figs. 1B–5B).

The 5-mm-long (0.7-mm-high) keloid was fully encased within the 1.5-mm-thick dermal layer. The top, bottom, and sides of the keloid were highly stressed by the traction (red), but the pulled end demonstrated relatively low stress (green) (Fig. 1B). The surrounding tissues did not show strong stress (pale light orange) (Fig. 1A).

Given that the 10-mm-long keloid was 1.4-mm high, it remained just within the boundaries of the dermis. The stress was distributed relatively evenly all over the keloid (Fig. 2B). However, the dermis that lay immediately adjacent to the keloid now showed middle stress (light orange). By contrast, the epidermis above the keloid and the subcutaneous tissue below exhibited low stress (light blue and dark blue, respectively) (Fig. 2A).

The 15-mm-long (2.1-mm-high) keloid is revealed beyond the surface of the skin. The relatively high stress in the adjacent dermis had spread further (orange). The subcutaneous tissue below continued to show low stress (dark blue) (Fig. 3A). With regard to the keloid, the stress now tended to be distributed at the areas that lay at the boundaries of the dermis. The keloid top and bottom displayed relatively little stress (yellow) (Fig. 3B).

The 20-mm-long keloid demonstrated more pronounced upward swelling. The high stress in the shallow dermis at the margin and the low stress in the underlying subcutaneous tissue had spread further (orange and dark blue, respectively). The top of the keloid now demonstrated mild compressive stress (yellow-green) (Fig. 4A). With regard to the keloid body, the center displayed mild stress (yellow-green). The high stress was now concentrated at the tractioned end, including at the adjacent keloid sides that lay at the shallow dermis (red) (Fig. 4B).

The patterns seen in the 20-mm-long keloid were even more pronounced in the 50-mm-long keloid. Thus, the stress of the surrounding dermis had spread hugely (reddish-orange), and there was pronounced low stress on the underlying subcutaneous tissue (dark blue) and the top of the keloid (light blue) (Fig. 5A). Moreover, the top and bottom of the keloid displayed low stress (light blue and yellow-green, respectively) and the high stress had focused in a tight band at the tractioned end (red) (Fig. 5B).

Figures 1A–5A show the locations in each keloid that bore maximum and minimum stress. These values were plotted against keloid size in Figure 6. This showed that with increasing size, the minimum stress dipped slightly at 10 mm, recovered, and then dropped mildly. Conversely,

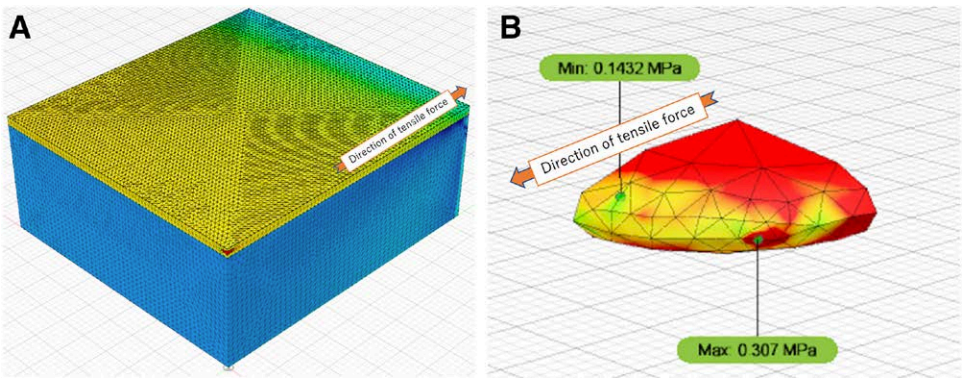

Fig. 1. FEA of the ellipsoid keloid that was 5 mm in long axis. The keloid was embedded in the dermis of normal skin and subjected to 100 N traction. The stress on the surrounding skin layers (A) and the keloid itself (B) was visualized.

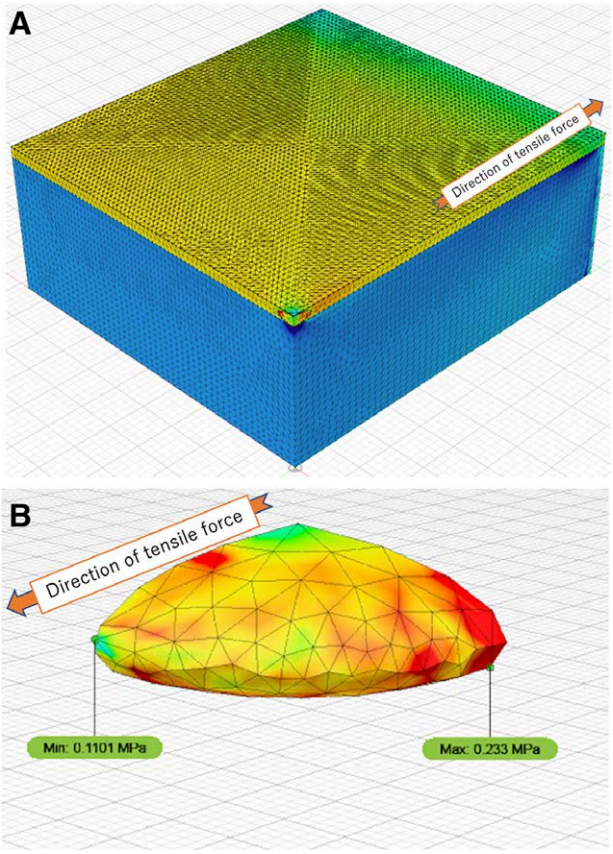

Fig. 2. FEA of the ellipsoid keloid that was 10 mm in long axis. The keloid was embedded in the dermis of normal skin and subjected to 100 N traction. The stress on the surrounding skin layers (A) and the keloid itself (B) was visualized.

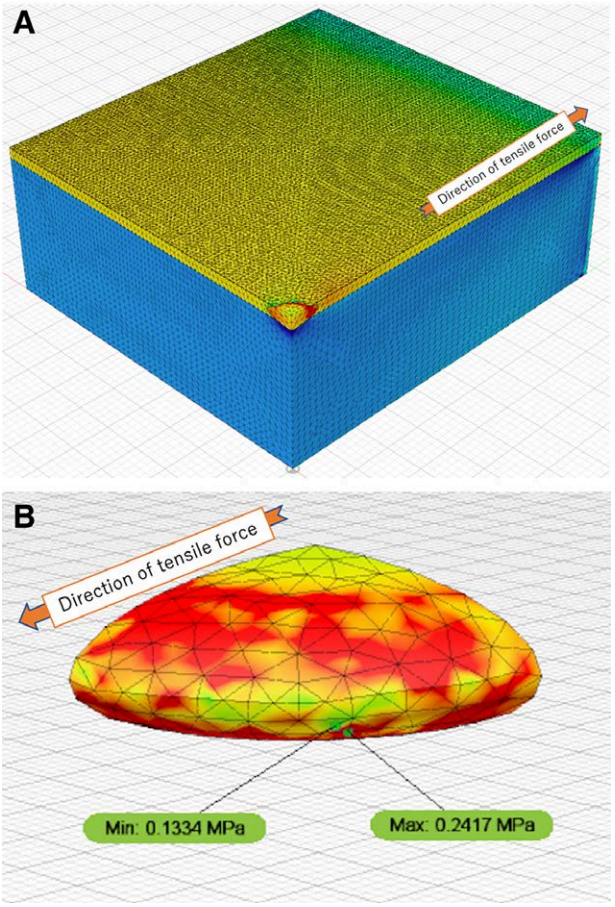

Fig. 3. FEA of the ellipsoid keloid that was 15 mm in long axis. The keloid was embedded in the dermis of normal skin and subjected to 100 N traction. The stress on the surrounding skin layers (A) and the keloid itself (B) was visualized.

although the maximum stress also dipped slightly at 10 mm (0.233 MPa), it rose linearly to 0.3967 MPa in the 50-mm-long keloid (Fig. 6).

Analysis of the Long and Short Diameters of Acne-derived Keloids

We retrieved clinical photographs of 220 physically isolated, erythematous, elevated, chest/shoulder/back acne keloids of 47 patients. The patients were mostly men (79%) and their mean age was 30 (range, 16–67) years. Of the 220 keloids, 81 and 139 were on the chest and shoulder/back, respectively. The regression analysis showed that the 2 dimensions were positively correlated (coefficient of determination $R^2 = 0.496$) with an estimated regression of $y = 0.1581x + 4.4493$ (where x is the long diameter and y is the short diameter) (Fig. 7A). Estimate of regression coefficient was statistically significant ($b = 3.14$, SE = 0.21, $t = 14.65$, $P < 0.05$). Notably, χ_1^2 test showed that small keloids measuring ≤5 mm tended to be circular: 16, 10, and 14 measured 3 × 3, 4 × 4, and 5 × 5 mm, respectively ($\chi_1^2 = 103.53$, $P < 0.05$) (Fig. 7B).

Pathological Study

Light microscopy of the toluidine blue–stained specimens showed that there were few blood vessels in the surrounding skin, including in the papillary and reticular layers of the dermis (Fig. 8A). By contrast, many neovascular vessels were observed in the papillary dermal layer, but not the reticular dermal layer, of the keloid margin (Fig. 8B). In the keloid center, the boundary between the papillary and reticular layers of the dermis became unclear, and the dermis was covered with keloidal collagen (Fig. 8C).

Electron microscopy showed that in the surrounding skin, fragments of keratinocyte, fibrin, and numerous cell fragments were observed just below the epidermal basement membrane (Fig. 9A). In the keloid margin, many cells and blood vessels were observed just below the epidermal basement membrane (Fig. 9B). Degenerated fibroblast-like cells, indicated by swollen mitochondria, were observed in the papillary layer of the dermis. These cells were surrounded by fibrin derived from blood vessels (Fig. 9C). In the keloid center, myofibroblasts with large irregular nuclei and abundant actin filaments were observed. These myofibroblasts contained fibronexus, myofilaments, and dense bodies, and produced collagen fibers (Fig. 9D).

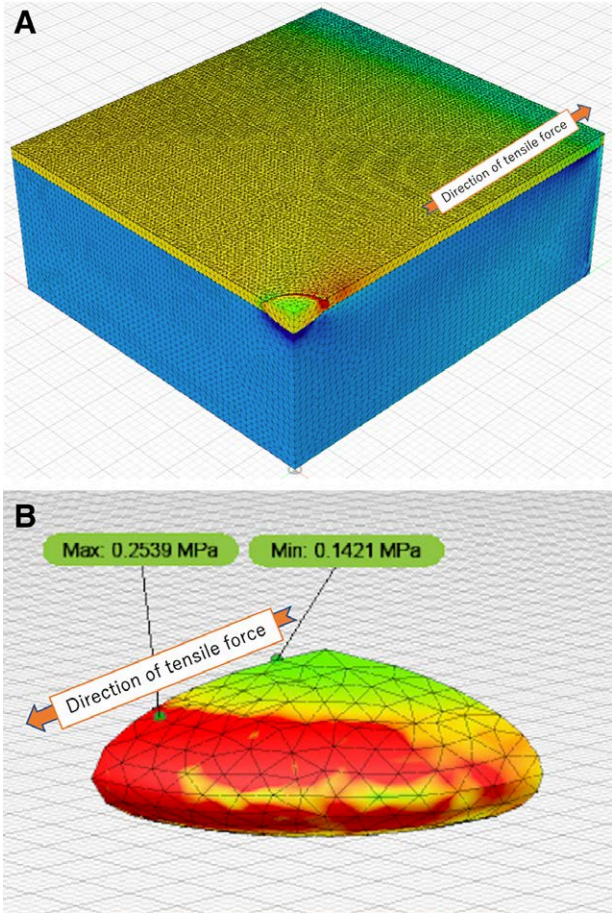

Fig. 4. FEA of the ellipsoid keloid that was 20 mm in long axis. The keloid was embedded in the dermis of normal skin and subjected to 100 N traction. The stress on the surrounding skin layers (A) and the keloid itself (B) was visualized.

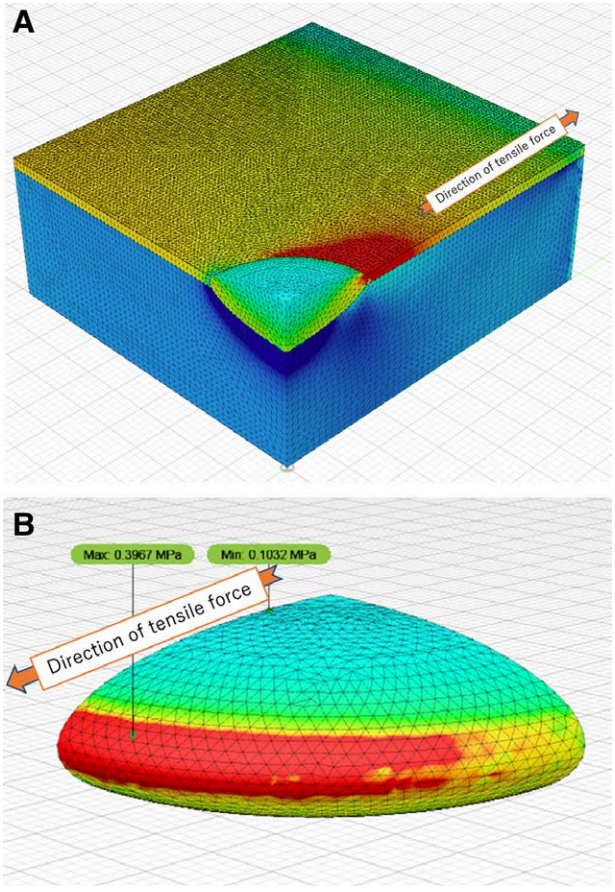

Fig. 5. FEA of the ellipsoid keloid that was 50 mm in long axis. The keloid was embedded in the dermis of normal skin and subjected to 100 N traction. The stress on the surrounding skin layers (A) and the keloid itself (B) was visualized.

DISCUSSION

The present FEA study showed that the same traction force on differently sized but identically shaped keloids led to quite different stress distributions on the keloid. Thus, as the keloid "grew" from being encased completely in the dermis to breaching the dermis and growing upward, the traction induced first central stress, then evenly distributed stress, increasing focalization of the stress at the pulled end and the adjacent sides at the border between the epidermis and dermis. It shows that this change starts after the keloid breaches the dermis: in our model, this occurred with 15-mm or longer (2.1-mm-high) keloids.

Thus, the round acne keloids are likely to start elongating in response to mechanical stress after they have expanded beyond the dermal tissue. This is consistent with our measurements of acne keloids: these keloids tended to remain round until they achieved a diameter of 4–5 mm, at which point they demonstrated increasing elongation. This is well visualized in the graph in Figure 7. This is consistent with the estimated regression: the estimated intercept is 4.4493, which indicates that the keloid starts to elongate when it becomes 4–5 mm in diameter.

Our FEA also showed that after the elongation event, the stress in the center of the keloid body, well beyond the skin surface, is lower, and the stress in the subcutaneous tissue below the keloid is rather lower. This is presumably due to the stiffness of the body of the keloid models and the fact that the main areas of traction of the models are the epidermis and dermis portions. This is consistent with clinical observations showing that the center of a keloid tends to flatten and that acne keloids generally do not extend to the fascia.

Our FEA also showed that as the keloid "grew," there was initially low stress on the surrounding tissues, but this then changed to high stress in the dermal margin, especially the surface of the skin. These changes are associated with decreasing stress on the underlying subcutaneous tissue and, later, with decreasing stress on the top of the keloid. The stress in the dermal margins appeared when the keloid was about to breach the dermis. Thus, the keloid elongation event is preceded by stress in the adjacent upper skin layers, which expands as the keloid grows. Indeed, our microscopy analyses showed that the surrounding skin of

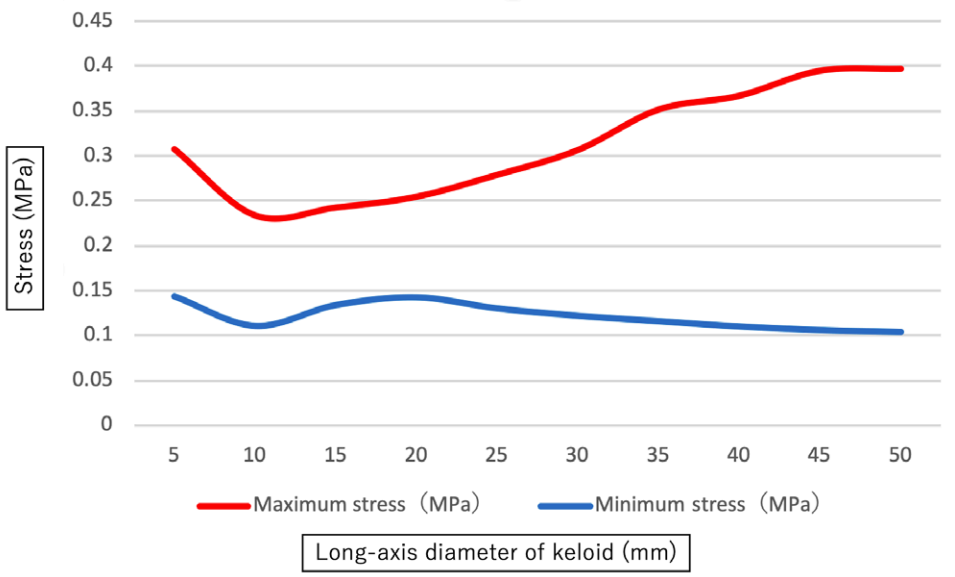

Fig. 6. Change in the maximum and minimum stress values recorded by FEA as the keloid model "grew." The maximum (red) and minimum (blue) stress values recorded for each of the 10 differently sized keloids (see values in Figs. 1B–5B) were plotted against keloid size.

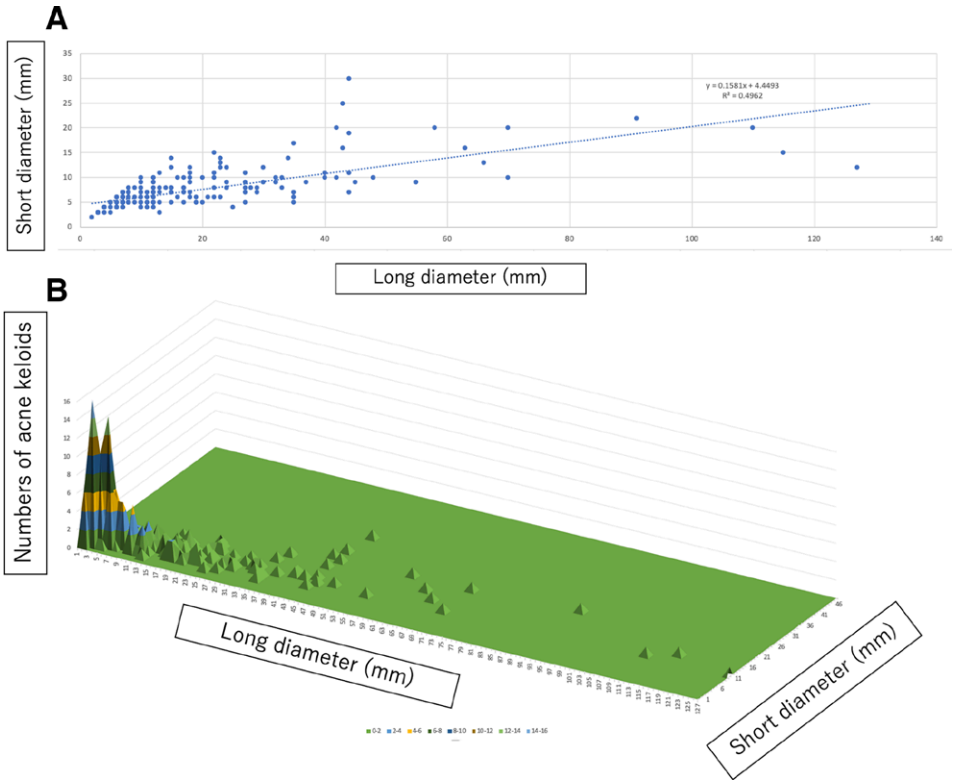

Fig. 7. Correlation between the long and short diameters of acne keloids, as determined from clinical photographs. The dimensions of 220 erythematous, elevated, and spatially distanced acne keloids on the chest, back, and shoulder of 47 patients were measured. A, Two-dimensional scatterplots with long and short diameters on the horizontal and vertical axes. Regression analysis was conducted. B, Contour lines to visualize the number of pieces of each size.

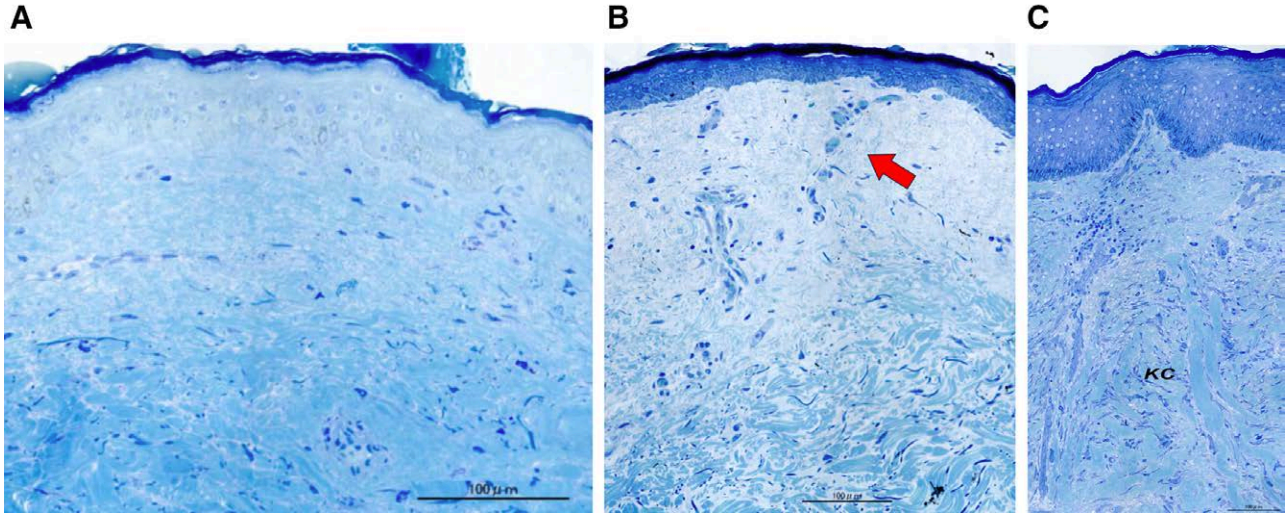

Fig. 8. Toluidine blue–stained image of surrounding skin, leading margin, and the center of an excised acne keloid on the chest. A, The surrounding tissues show few blood vessels in the papillary layer of the dermis. Bar, 100 μm. B, The leading keloid margin shows many blood vessels (red arrow) under the papillary layer of the dermis. The dermal reticularis resembles that of the surrounding tissue. Bar, 100 μm. C, The central region shows the blurring of the boundary between the papillary dermis and the reticularis layer. KC signifies the blue-stained fibrous keloidal collagen bundles, which extend into the deeper layers. Bar, 100 μm.

chest acne keloids displays signs of stress, namely, cell fragments and fibrin. This is consistent with our studies showing that stress induces inflammation, which spills over into the adjacent tissue in the direction of stress.

This was consistent with our FEA, which showed that as the keloid "grew," the stress induced by traction increasingly concentrated in the upper dermis at the leading keloid edge. It is also consistent with our animal experiments, which showed that stress increases vascular permeability.[25] However, the fact that increased vascularity was not observed in the surrounding skin suggests that keloids do not occur when normal skin is subjected to stress; rather, they require a trigger (eg, wounding or acne vulgaris) that reaches the reticular layer.

Our findings have 2 clinical implications. First, the fact that acne keloids remain round until a diameter of 4–5 mm but then start rapidly elongating supports the notion that to obtain good results, acne keloid treatment should start while the lesions are small. Second, given that keloid growth is associated with increased stress in the shallow dermis of the keloid margins, and stress induces inflammation,[11] it is confirmed that early treatment with steroid tape is fully effective.[26–28]

Finally, the fact that the stress in the keloid decreases after the keloid begins to elongate supports the notion that keloid is a stress-responsive fibroproliferative disease rather than a tumor, which grows essentially in all directions. This adds to the increasing body of evidence that suggests that although keloids bear some features of tumors, they also have many characteristics that are not consistent with tumors.

Study Limitations

The FEA modeled the 10 keloids as identically shaped ellipsoids that varied only in size and that were subjected to a single traction force of the same strength and coming from the same direction. This simplified setting thus does not account for the many variables that affect keloid growth, which include race, age, gender, body shape, thickness of each skin structure, elasticity, adhesion to subcutaneous structures, the type of joint movements that predominate at each site, and respiratory movement. Moreover, the model did not account for the changes within the keloid as it spreads into the surrounding skin: these changes are exemplified by our microscopy images. In addition, the proinflammatory effect of keloid elongation on the surrounding tissues was not accommodated in our FEA, nor did we examine the effect of different keloid shapes or closely adjacent keloids on keloid growth.

CONCLUSIONS

Our FEA, clinical data, and specimen pathology analyses showed that acne keloids remain round until they grow to 4–5 mm in diameter; thereafter, they elongate rapidly in the predominant direction of tractional stress. Moreover, tractional stress is focused on the shallow dermis of the keloid at its leading margin. In addition, the stress of the top/bottom of the keloid body and surrounding tissues decreases as the keloid starts to elongate. These findings suggest that keloid-prone acne should be treated with steroid tape or other keloid therapy when it reaches 4–5 mm in diameter.

Nobuaki Ishii, MD
Department of Plastic Surgery
Nippon Medical School Chibahokusoh Hospital
1715 Kamakari, Inzai City
Chiba Prefecture 270-1694, Japan
E-mail: s8006@nms.ac.jp

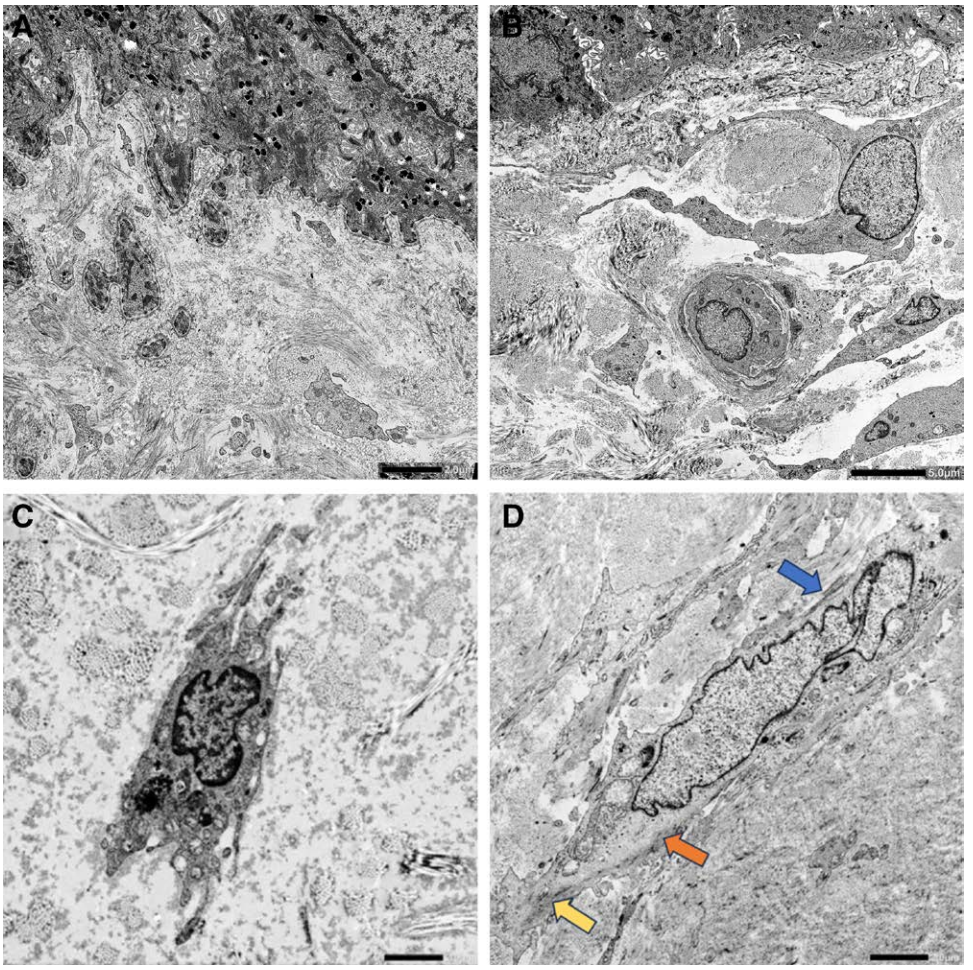

Fig. 9. Electron microscopy of the surrounding skin, leading margin, and the center of an excised acne keloid on the chest. A, The surrounding tissue shows keratinocyte fragments, fibrin, and numerous cell fragments just below the epidermal baseplate and breaking through the basement membrane. Bar, 2.0 μm. B, In the keloid margin, many cells and blood vessels were observed just below the epidermal basement membrane. Bar, 5.0 μm. C, In the keloid margins also show fibroblast-like cells in the papillary dermis, surrounded by fibrin. Bar, 2.0 μm. D, The central region shows myofibroblasts characterized by an irregular nucleus and intracellular actin filament fibers. They are proliferating actively and surrounded by fibronexus (blue arrow), myofilaments (orange arrow), and dense bodies (yellow arrow). Bar, 2.0 μm.

DISCLOSURE

The authors have no financial interest to declare in relation to the content of this article.

REFERENCES

1. Marneros AG, Krieg T. Keloids-clinical diagnosis, pathogenesis, and treatment options. *J Dtsch Dermatol Ges.* 2004;2:905–913.
2. Nakashima M, Chung S, Takahashi A, et al. A genome-wide association study identifies four susceptibility loci for keloid in the Japanese population. *Nat Genet.* 2010;42:768–771.
3. Gurtner GC, Werner S, Barrandon Y, et al. Wound repair and regeneration. *Nature.* 2008;453:314–321.
4. Ogawa R, Watanabe A, Than Naing B, et al. Associations between keloid severity and single-nucleotide polymorphisms: importance of rs8032158 as a biomarker of keloid severity. *J Invest Dermatol.* 2014;134:2041–2043.
5. Shih B, Garside E, McGrouther DA, et al. Molecular dissection of abnormal wound healing processes resulting in keloid disease. *Wound Repair Regen.* 2010;18:139–153.
6. Ogawa R, Okai K, Tokumura F, et al. The relationship between skin stretching/contraction and pathologic scarring: the important role of mechanical forces in keloid generation. *Wound Repair Regen.* 2012;20:149–157.
7. Dohi T, Miyake K, Aoki M, et al. Tissue inhibitor of metalloproteinase-2 suppresses collagen synthesis in cultured keloid fibroblasts. *Plast Reconstr Surg Glob Open.* 2015;3:e520.
8. Aoki M, Miyake K, Ogawa R, et al. siRNA knockdown of tissue inhibitor of metalloproteinase-1 in keloid fibroblasts leads to degradation of collagen type I. *J Invest Dermatol.* 2014;134:818–826.
9. Lancerotto L, Orgill DP. Mechanoregulation of angiogenesis in wound healing. *Adv Wound Care (New Rochelle).* 2014;3:626–634.
10. Jumper N, Hodgkinson T, Paus R, et al. Site-specific gene expression profiling as a novel strategy for unravelling keloid disease pathobiology. *PLoS One.* 2017;12:e0172955.
11. Ogawa R, Akaishi S, Huang C, et al. Clinical applications of basic research that shows reducing skin tension could prevent and treat abnormal scarring: the importance of fascial/ subcutaneous tensile reduction sutures and flap surgery for keloid and hypertrophic scar reconstruction. *J Nippon Med Sch.* 2011;78:68–76.

12. Agha R, Ogawa R, Pietramaggiori G, et al. A review of the role of mechanical forces in cutaneous wound healing. *J Surg Res*. 2011;171:700–708.
13. Schneider L, Warren S. The relationship between keloid growth pattern and stretching tension –visual analysis using the finite element method : a brief history of keloids. *Ann Plast Surg*. 2008;60:452–454.
14. Al-Attar A, Mess S, Thomassen JM, et al. Keloid pathogenesis and treatment. *Plast Reconstr Surg*. 2006;117:286–300.
15. Ogawa R. Mechanobiology of scarring. *Wound Repair Regen*. 2011;19:s2–s9.
16. Huang C, Holfeld J, Schaden W, et al. Mechanotherapy: revisiting physical therapy and recruiting mechanobiology for a new era in medicine. *Trends Mol Med*. 2013;19:555–564.
17. Huang C, Akaishi S, Ogawa R. Mechanosignaling pathways in cutaneous scarring. *Arch Dermatol Res*. 2012;304:589–597.
18. Akaishi S, Akimoto M, Ogawa R, et al. The relationship between keloid growth pattern and stretching tension. *Ann Plast Surg*. 2008;60:445–451.
19. Nagasao T, Aramaki-Hattori N, Shimizu Y, et al. Transformation of keloids is determined by stress occurrence patterns on perikeloid regions in response to body movement. *Med Hypotheses*. 2013;81:136–141.
20. Dohi T, Padmanabhan J, Akaishi S, et al. The interplay of mechanical stress, strain, and stiffness at the keloid periphery correlates with increased caveolin-1/ROCK signaling and scar progression. *Plast Reconstr Surg*. 2019;144:58e–67e.
21. Balko B, Berger RL. A direct finite element analysis method for particle mechanics: the three-body problem. *Curr Mod Biol*. 1969;3:110–121.
22. Kurokawa I, Nakase K. Recent advances in understanding and managing acne. *F1000Res*. 2020;9:F1000.
23. Lee Y, Hwang K. Skin thickness of Korean adults. *Surg Radiol Anat*. 2002;24:183–189.
24. Chow WW, Odell EI. Deformations and stresses in soft body tissues of a sitting person. *J Biomech Eng*. 1978;100:79–87.
25. Demir T, Takada H, Furuya K, et al. Role of skin stretch on local vascular permeability in murine and cell culture models. *Plast Reconstr Surg Glob Open*. 2022;10:e4084.
26. Goutos I, Ogawa R. Steroid tape: a promising adjunct to scar management. *Scars Burn Heal*. 2017;3:2059513117735483.
27. Ogawa R, Akita S, Akaishi S, et al. Diagnosis and treatment of keloids and hypertrophic Scars—Japan Scar Workshop Consensus Document 2018. *Burns Trauma*. 2019; 7:39.
28. Ogawa R, Quong WL. Effective treatment of an aggressive chest wall keloid in a woman using deprodone propionate plaster without surgery, radiotherapy, or injection. *Plast Reconstr Surg Glob Open*. 2024;12:e6117.